Theoretical Study on the Phenyl Torsional Potentials of *trans*-Diphenyldiphosphene

Yoshiaki Amatatsu[†]

Faculty of Engineering and Resource Science, Akita University, Tegata Gakuen-cho, Akita 010-8502, Japan

Received: May 19, 2008; Revised Manuscript Received: June 26, 2008

The phenyl torsional potentials of *trans*-diphenyldiphosphene (*trans*-phosphobenzene; *t*-DPP), which is an analogue of *trans*-azobenzene (*t*-AZB), have been examined by means of ab initio complete active space self-consistent field (CASSCF) calculations. Though the electronic structures of *t*-DPP are similar to those of *t*-AZB, the phenyl torsional potentials are different from each other. In S_0, the potential energy curve of *t*-DPP has double minima at nonplanar conformations with C_2 and C_i symmetries, while that of *t*-AZB has only minimum at a planar conformation with C_{2h}. In S_1, the phenyl torsion of *t*-AZB is impeded from a planar geometry more than that in S_0. On the other hand, the phenyl torsion of *t*-DPP is promoted so that the phenyl groups are perpendicularly twisted against the P═P double bond around the Franck−Condon region. Comments on the experimental findings of realistic diphosphenes protected by bulky substituents are also made.

1. Introduction

Multiplebonds compounds of heavier group 15 elements are of great interest in basic chemistry as well as material science. Since the first report of diphosphene of which the P═P double bond is kinetically protected by a bulky substituent in 1981,[1] the synthesis, the structures and the reactivity of various double bond compounds of heavier group 15 elements have been examined[2−6] and reviewed as well.[7−9] In accordance with realization of this class of compounds, theoretical investigations of the bonding nature and the reactivity of heavier group 15 element compounds have been done, although the oversimplified molecules without substituents were adopted as model compounds in most of calculations[6,10−14]

In the past several years, a new direction, where P═P double bond compounds are intended to be utilized as photofunctional materials of electronic, optical, and magnetic devices, has begun to grow. Yoshifuji and co-workers systematically examined the electronic effects of the substituents on diphosphenes.[15] Thereby, they pointed out that the electron-donating substituent at the para position enhances the reactivity of the P═P double bond of diphosphenes protected by bulky substituent. In other words, the reactivity of diphosphene can be controlled by an effective substituent thermodynamically as well as kinetically. Poly(*p*-phenylenevinylenes) (PPVs) are useful π conjugated polymers for devices. Protasiewicz and Simpson synthesized a diphosphene−PPV unit containing a P═P bond.[16] The basic idea of these applications to new materials is based on the fact that the P═P compounds give rise to visible absorption due to small HOMO−LUMO gaps so as to be suitable for photofunctional molecular devices To exploit excellent photofunctional molecules, however, characterization of the excited states of P═P compounds is desirable. A conventional UV−vis absorption spectrum gives us information on the electronic structures of the low-lying excited states assigned to n−π^* and $\pi-\pi^*$, respectively.[17,18] On the benefit of the resonance Raman excitation spectrum by Copeland et al., it is found that the geometry in $\pi-\pi^*$ is very different from that of the ground state, while that in n−π^* is similar to that in the ground state.[18] Unfortunately, however, there is still little information on the excited states of the P═P compounds so as to exploit new excellent photofunctional materials. Therefore our purpose is to clarify the P═P double bond character in the excited states and to give guidelines for molecular design of photofunctional P═P compounds from a theoretical side.

In the present study, we take *trans*-diphenyldiphosphene (*trans*-phosphobenzene; *t*-DPP), which is an analogue of *trans*-azobenzene (*t*-AZB), as a model P═P compound and compare the S_1-state character of *t*-DPP with that of *t*-AZB around the Franck−Condon region.

2. Method of Calculations

DPP has the seven π-type occupied orbitals and the corresponding unoccupied π^* orbitals, as well as two nonbonding orbitals on the P atoms. However, CASSCF calculations, which allow all possible excitations from the nine occupied orbitals to the lowest seven unoccupied ones (i.e., 18 electrons in 16 orbitals CASSCF denoted by (18,16)CASSCF), are quite unrealistic to scan the global potential energy surfaces for the photochemistry of DPP. So reduction of active space is important. Preliminarily we did configuration interaction (CI) calculations where up to the triple excitations from the closed-shell Hartree−Fock configuration were taken into account. On the basis of the preliminary CI calculations, the highest five π occupied and the lowest five π^* unoccupied orbitals as well as two nonbonding orbitals on the P atoms are enough to describe our present interest of S_0 and S_1 states at any geometries which possibly contribute to the photochemistry of DPP. Therefore we adopted 14 electrons in 12 orbitals CASSCF ((14,12)CASSCF) for scanning of the global potential energy surfaces. In necessity, we made correction for the (14,12)CASSCF energy of each electronic state using second-order multireference Möller−Plesset perturbation (MRMP2) method where all valence and virtual orbitals were included.

We first optimized the geometries in S_0 (S_0-geometry) by means of a state-specific[14,12] CASSCF. Then we calculated the phenyl torsional potentials in S_0 and S_1 in the region of *t*-DPP under constraint of C_2 and/or C_i symmetry. We also did similar calculations of *t*-AZB by (14,12)CASSCF and MRMP2 methods.

[†] Fax: 81-18-889-2601. E-mail: :amatatsu@ipc.akita-u.ac.jp.

10.1021/jp8043972 CCC: $40.75
Published on Web 08/26/2008

TABLE 1: Characteristic Optimized Parameters at Important Conformations of *t*-DPP and *t*-AZB

	S_0-geometry	S_0-geometry (C_{2h}) [a]	S_1-geometry	S_1-geometry (C_{2h}) [a]
DPP				
bond distances (Å)				
$P^{\alpha}P^{\beta}$	2.056 (2.056)[b]	2.052	2.153 (2.153)[c]	2.122
$P^{\alpha}C^{1}$, $P^{\beta}C^{1'}$ [d]	1.834 (1.834)	1.835	1.821 (1.821)	1.805
bond angles (deg)				
$\alpha(C^{1}P^{\alpha}P^{\beta})$, $\beta(C^{1'}P^{\beta}P^{\alpha})$ [d]	103.1 (103.3)	104.5	109.0 (109.1)	112.7
dihedral angles (deg)				
$\tau(C^{1}P^{\alpha}P^{\beta}C^{1'})$	−177.9 (180.0)	180.0	−179.1 (180.0)	180.0
$\phi(C^{2}C^{1}P^{\alpha}P^{\beta})$, $\phi'(C^{2'}C^{1'}P^{\beta}P^{\alpha})$ [d]	30.3 (30.0)	0.0	89.6 (88.6)	0.0
AZB[e]				
bond distances (Å)				
$N^{\alpha}N^{\beta}$	1.246		1.257	
$N^{\alpha}C^{1}$, $N^{\beta}C^{1'}$	1.426		1.369	
bond angles (deg)				
$\alpha(C^{1}N^{\alpha}N^{\beta})$, $\beta(C^{1'}N^{\beta}N^{\alpha})$	114.8		128.4	
dihedral angles (deg)				
$\tau(C^{1}N^{\alpha}N^{\beta}C^{1'})$	180.0		180.0	
$\phi(C^{2}C^{1}N^{\alpha}N^{\beta})$, $\phi'(C^{2'}C^{1'}N^{\beta}N^{\alpha})$	0.0		0.0	

[a] The values are the optimized parameters under constraint of C_{2h} symmetry. [b] The values in parentheses are the optimized parameters under constraint of C_i symmetry. The energy with the C_i geometry in S_0 is higher only by 0.015 eV than that of the most stable S_0-geometry with C_2 symmetry. [c] The values in parentheses are the optimized parameters under constraint of C_i symmetry. Considering that the phenyl groups are almost perpendicularly twisted and the energy difference of S_1-geometries with C_2 and C_i symmetry is only by 0.001 eV, S_1-geometry with C_i symmetry is substantially the same as S_1-geometry with C_2 symmetry. [d] Due to the C_2 or C_i symmetry, the bond distances, and bond angles, take the same values. The only difference is the sign of the dihedral angles (ϕ, ϕ') of C_i geometry. [e] S_0- and S_1-geometries of AZB have C_{2h} symmetry.

TABLE 2: Standard Bond Distances Bonded to a P Atom

molecule	bond	bond distance[a]
PH═PH	P═P	2.039 (2.002)
PH_2-PH_2	P−P	2.206 (2.214)
CH_2═PH	C═P	1.678 (1.653)
CH_3-PH_2	C−P	1.860 (1.857)

[a] The values are fully optimized by the second order Möller−Plesset perturbation method with the same basis set in the present study, while those in the parentheses are fully optimized by the restricted Hartree−Fock method.

TABLE 3: Electronic Structures of *t*-DPP at S_0-Geometry

	excitation energy (eV)	dipole moment (D)	main CSFs[a]
S_0	0.0 (0.0)[b]	0.025	0.897 (closed shell)
S_1	3.544 (2.759)	0.088	0.901 (n_+-π^*) [c]

[a] The CSFs (configuration state functions) of which absolute values of CI coefficients are greater than 0.3 are listed. [b] The values in the parentheses are obtained by MRMP2 corrections. [c] The relevant MOs in the parentheses are shown in Figure 2.

We used the GAMESS program in the present ab initio calculations with Huzinaga−Duunning double-ζ basis set augmented by polarizations ($\alpha_d = 0.75$ for C atoms, $\alpha_d = 0.55$ for P atoms, and $\alpha_d = 0.80$ for N atoms).[19]

3. Results and Discussion

3.1. Geometrical Feature of S_0-Geometry. First of all we mention the geometrical feature of S_0-geometry. Table 1 lists the characteristic optimized parameters at S_0-geometry as well as those at other key conformations. The most characteristic feature of *t*-DPP at S_0-geometry is a nonplanar structure with C_2 (or C_i symmetry). Regarding the bond distances, the PP bond (2.056 Å) has double bond character (refer to Table 2 about standard bond distances bonded to P atom). The linkage PC bonds (1.834 Å) have a single bond character. Tentatively we optimized the geometry in S_0 under constraint of C_{2h} symmetry. As seen in Table 1, the optimized parameters except for the torsional angles are very similar to those at S_0-geometry. This implies that there is little π conjugation between the phenyl groups and the P═P part even at a planar conformation in S_0. Therefore the main factor of the nonplanarity of S_0-geometry is electronic repulsion between the P═P part and the phenyl groups. The single bond character of the linkage PC bonds make it possible to escape from steric repulsion between the P═P part and the bulky substituents. In real diphosphenes which are protected by bulky substituents, the phenyl torsional angles ϕ,

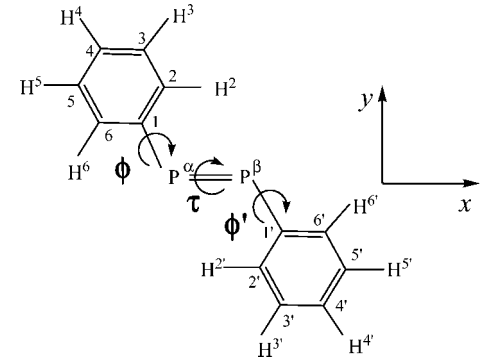

Figure 1. Numbering of atoms in DPP. The bending angles of $C^{1}P^{\alpha}P^{\beta}$ and $C^{1'}P^{\beta}P^{\alpha}$ are denoted by α and β. The dihedral angles of $C^{1}P^{\alpha}P^{\beta}C^{1'}$, $C^{2}C^{1}P^{\alpha}P^{\beta}$, and $P^{\alpha}P^{\beta}C^{1'}C^{2'}$ are denoted by τ, ϕ, and ϕ'. A similar definition of the numbering of atoms in AZB is also made. The *z*-axis is perpendicular to the *xy*-plane.

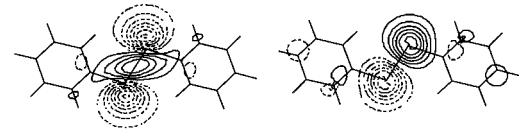

Figure 2. Molecular orbitals relevant to the S_0 and S_1 states at S_0-geometry of *t*-DPP. The other nonbonding orbital (n_-), which is an approximately antisymmetric linear combination of the lone pair orbital on the P atoms, is much less important.

TABLE 4: Electronic Structures of *t*-AZB at S_0-Geometry

	excitation energy (eV)	dipole moment (D)	main CSFs[a]
S_0	0.0 (0.0)[b]	0.000	0.907 (closed shell)
S_1	3.277 (2.412)	0.000	0.896 (n_+-π^*)[c]

[a] The CSFs of which absolute values of CI coefficients are greater than 0.3 are listed. [b] The values in the parentheses are obtained by MRMP2 corrections. [c] The relevant MOs in the parentheses are shown in Figure 3.

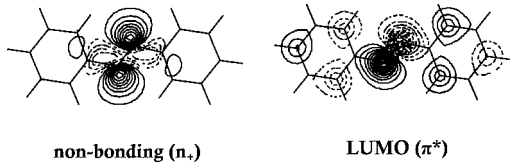

Figure 3. Molecular orbitals relevant to the S_0 and S_1 states at S_0-geometry of *t*-AZB. The other nonbonding orbital (n_-), which is an approximately antisymmetric linear combination of the lone pair orbital on the N atoms, is much less important.

ϕ' are almost 90°,[1,5] which is due to steric repulsion in addition to electronic repulsion.

Contrary to the stable nonplanar conformation of *t*-DPP, *t*-AZB takes a planar conformation with C_{2h} (see the relevant part of Table 1). The NC bonds (1.426 Å) slightly shrink due to somewhat resonance between the N═N part and the phenyl groups so that a planar conformation is more stable in S_0.

3.2. Electronic Structures at S_0-Geometry. Table 3 presents the electronic structures at S_0-geometry. Figure 2 shows the relevant molecular orbitals (MOs) to describe the electronic structures: the nonbonding MO and the lowest unoccupied MO (LUMO). The nonbonding MO mainly originates from symmetric linear combination of the lone pair orbitals on the P atoms, so we denote the symmetric nonbonding orbital by n_+ hereafter. The CASSCF excitation energy (3.544 eV) is higher than the experimental absorption maximum of the $n_+-\pi^*$ band (2.695 eV, i.e., ca. 460 nm), but the MRMP2 energy (2.759 eV) well reproduces the experimental one.[17,18] The electronic structure of *t*-DPP is found to be similar to those of *t*-AZB, as seen from Table 4 and Figure 3.

3.3. Phenyl Torsional Potentials around S_0-Geometry. Figures 4 and 5 present the phenyl torsional potentials of *t*-DPP and *t*-AZB, respectively. As seen in Figure 4a, the phenyl torsional potential curve of *t*-DPP in S_0 has double wells of which minima are $\phi = \phi' = 30.3°$ (for C_2) and $\phi = -\phi' = 30.0°$ (for C_i), respectively. On the other hand, the phenyl torsional potential curve of *t*-AZB has only a minimum at $\phi = 0°$ (see Figure 4b). This difference can be derived from the characters of the PC and NC linkage bonds. The PC bond distances of S_0^{opt} in Figure 4a (1.833−1.844 Å) are a normal P−C single bond irrespective of ϕ. On the other hand, the NC bond distances of S_0^{opt} in Figure 4b (1.426−1.436 Å) are shorter than a normal N−C single bond, which is due to resonance between the two phenyl groups and the N═N part. So the phenyl torsion of *t*-AZB is impeded from the planar S_0-geometry.

The phenyl torsional potentials in S_1 are much more different from each other. In case of *t*-AZB (see Figure 5b), the phenyl torsional potential becomes more stiff around $\phi = 0°$ (i.e., S_0-geometry) than that in S_0. Here we note that the energy scale in Figure 5b is double that in Figure 4b. The stiffness of the torsional potential can be interpreted as the fact that the NC linkage bonds increase the double bond character upon $n-\pi^*$ excitation in S_1 (for instance, refer to the $N^{\alpha}C^1$ and $N^{\beta}C^{1'}$ bond distances of S_0- and S_1-geometries (i.e., 1.426 and 1.369 Å) in Table 1). In the case of *t*-DPP, the phenyl torsion is promoted

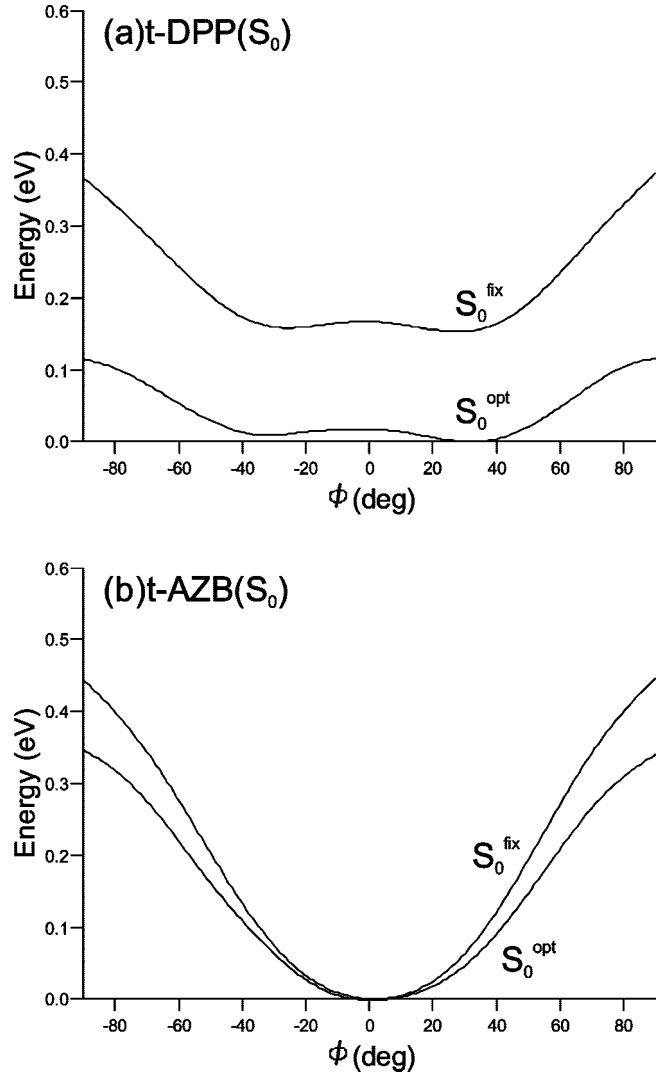

Figure 4. Phenyl torsional potentials in S_0 of (a) *t*-DPP and (b) *t*-AZB. The energies are relative to those at respective S_0-geometries. The positive values in the abscissa means $\phi' = \phi$ with C_2 symmetry, while the negative values means $\phi' = -\phi$ with C_i symmetry. The curves of S_0^{fix} are obtained as a function of ϕ, where the other parameters are fixed to those of S_0-geometries with C_{2h} symmetry. The curves of S_0^{opt} are obtained as a function of ϕ, where the other parameters are fully optimized.

up to $\phi \sim \phi' \sim 90°$. So our concern is why the phenyl groups are perpendicularly twisted against the P═P part for *t*-DPP to be stabilized in S_1 around the Franck−Condon region. One reason for the stability of the perpendicularly phenyl twisted conformation is that the PC linkage bonds hold a single bond character even in S_1 (refer to the $P^{\alpha}C^1$ and $P^{\beta}C^{1'}$ bond distances of S_1-geometry and S_1-geometry (C_{2h}; 1.821 and 1805 Å) in Table 1). However, this reason is not persuasive enough for the phenyl torsions to be promoted from $\phi \sim 30°$ to $\sim 90°$ in S_1. Another important factor for the stability at $\phi \sim 90°$ can be seen from Table 5. Upon electronic excitation into $S_1(n-\pi^*)$ at S_0-geometry, the electron populations of the in-plane orbitals (i.e., 3s, $3p_x$, $3p_y$) contributing to the nonbonding orbital decrease from 0.936, 1.065, 1.058 into 0.891, 0.828, 0.963, while that of the out-of-plane $3p_z$ orbital increases from 0.994 into 1.398 (refer to the values in the column of 30° in Table 5). It is also found that the electron population of the out-of-plane $3p_z$ orbital is almost constant in S_1 irrespective of ϕ. This means that the π electron is localized around the P═P part (refer to the π^* MO in Figure 2, for instance). Moreover, the net atomic charge

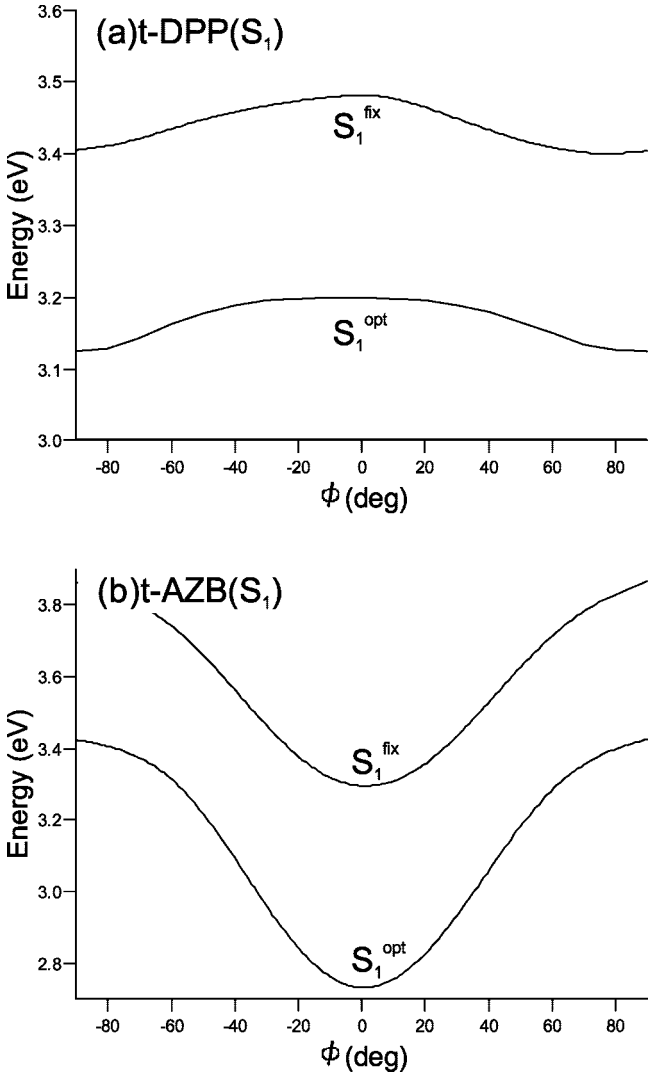

Figure 5. Phenyl torsional potentials in S_1 of (a) *t*-DPP and (b) *t*-AZB. The energies are relative to those at respective S_0-geometries. The meaning of the abscissa is same as that in Figure 4. The curves of S_1^{fix} are obtained as a function of ϕ, where the other parameters are fixed to those of S_0-geometries with C_{2h} symmetry. The curves of S_1^{opt} are obtained as a function of ϕ where τ is fixed to 180° and the other parameters are also fully optimized. Note that the energy scale of the ordinate in b is double those in Figure 4a,b and part a of this figure.

on the P atom is positive. In other words, the phenyl parts of *t*-DPP are negatively charged in S_1 as well as S_0. On the basis of these computational findings on the electron populations, the negatively charged phenyl groups avoid the electronic repulsion with the electron-rich π orbital of the P═P part in S_1 more preferably than in S_0. Therefore, the phenyl torsion is promoted in S_1 more than in S_0.

To deepen understanding on the P═P double bond character, we compare the electron populations with those of *t*-AZB. Table 6 lists the electron populations of *t*-AZB as a function of the phenyl torsional angle. Upon electronic excitation into S_1 at S_0-geometry (i.e., $\phi = 0°$), the electron populations of the in-plane orbitals (2s, $2p_z$, $2p_y$) decrease from 0.914, 1.158, 1.380 to 0.883, 1.050, 1.153, while that of the out-of-plane $2p_z$ orbital increases from 0.996 to 1.370. This is the same reason why the S_1 state is $n_+-\pi^*$. Contrary to the case of *t*-DPP, however, the electron population of the out-of-plane $2p_z$ orbital increases from 1.370 to 1.407 as ϕ increases. This can be interpreted as follow. The π conjugation between the N═N part and the two phenyl groups is enhanced in S_1, as mentioned above. So the phenyl torsion is more impeded due to the π conjugation in the NC linkage bonds. To energetically stabilize AZB in S_1 at a highly phenyl twisted conformation, the N═N part and the two phenyl groups turn to be off-resonant. As a result, the π electrons, which are delocalized between the N═N part and the phenyl groups at a planar conformation, are drawn back to the more electronegative N atom as ϕ increases. Actually, the increment of the electron population on the $2p_z$ (0.037, which is the difference of the values between 0° and 90° in Table 6) is almost the same as the increment of the negative charge on the N atom in S_1 (−0.036). In the case of *t*-DPP (see Table 5), on the other hand, the electron populations in the in-plane 3s and $3p_x$ increase from 0.886, 0.826 to 0.901, 0.838 in S_1 as ϕ increases. This increment (i.e., 0.015 + 0.012) is almost the same as the decrease of the net charge on the P atom (−0.030). In other words, the P═P part accepts the negative charge from the phenyl groups. Figure 6 presents the important MOs relevant to the S_1 state at ϕ = 90°. At the perpendicularly phenyl twisted conformation, the $n_+-\pi^*$ excitation is still the main one, but other MOs, in which another nonbonding orbital around the P═P bond (i.e., antisymmetric linear combination of lone pair orbitals on the P atoms denoted by n_-) and the π orbital over the phenyl groups mix up greatly, becomes important. These MOs make it possible that the charge over the phenyl groups transfers into the in-plane region around the P atoms. In the case of *t*-AZB, on the other hand, such charge transfer is much less important.

Before terminating this section, we make comment on the resonance Raman excitation profile, which implies that the distortion from the ground-state geometry is small upon $n_+-\pi^*$ excitation.[18] In their experiment, they used a P═P compound protected by a bulky substituent and so the two bulky substituents are perpendicularly twisted against the P═P double bond even in S_0. In S_1, as mentioned above, a perpendicularly phenyl twisted conformation is stable around the Franck−Condon region and the linkage PC bond holds a single bond character irrespective of the phenyl torsion and the electronic states (S_0 and S_1). So we also

TABLE 5: Torsional Angle (ϕ, deg) Dependence of Löwdin Charge Populations of *t*-DPP[a]

	charge population			
atomic orbitals on P [b]	$\phi = 0°$	$\phi = 30°$	$\phi = 60°$	$\phi = 90°$
3s	0.932, 0.886 [c]	0.936, 0.891	0.942, 0.898	0.945, 0.901
$3p_x$	1.066, 0.826	1.065, 0.828	1.064, 0.834	1.064, 0.838
$3p_y$	1.059, 0.964	1.058, 0.963	1.058, 0.962	1.063, 0.962
$3p_z$	1.000, 1.399	0.994, 1.398	0.980, 1.398	0.970, 1.398
net charge on P	0.246, 0.249 [d]	0.249, 0.242	0.254, 0.227	0.256, 0.219

[a] To see the phenyl torsional angle dependence only, the other parameters are fixed to those of S_0-geometry (C_{2h}). [b] The directions of *x*,*y*,*z*-axes are defined in Figure 1. So the $3p_x$ and $3p_y$ are in-plane p-type orbitals, while the $3p_z$ orbital is out-of-plane irrespective of ϕ. [c] The first and second values are the electron populations in S_0 and S_1, respectively. Because of the C_2 symmetry, the values on the P^α and P^β atoms are same. [d] The first and second values are the net charges on the P atom in S_0 and S_1, respectively.

TABLE 6: Torsional Angle (ϕ, deg) Dependence of Löwdin Charge Populations of *t*-AZB[a]

	charge population			
atomic orbitals on N [b]	$\phi = 0°$	$\phi = 30°$	$\phi = 60°$	$\phi = 90°$
2s	0.914, 0.883 [c]	0.916, 0.884	0.920, 0.885	0.920, 0.885
$2p_x$	1.158, 1.050	1.157, 1.050	1.156, 1.050	1.155, 1.050
$2p_y$	1.380, 1.153	1.382, 1.151	1.386, 1.150	1.391, 1.151
$2p_z$	0.996, 1.370	0.990, 1.379	0.976, 1.398	0.967, 1.407
Net charge on N	−0.049, −0.044 [d]	−0.045, −0.052	−0.037, −0.070	−0.034, −0.080

[a] To see the phenyl torsional angle dependence only, the other parameters are fixed to those of S_0-geometry. [b] The directions of *x*,*y*,*z*-axes are defined in Figure 1. So the $2p_x$ and $2p_y$ are in-plane 2p-type orbitals, while the $2p_z$ orbital is out-of-plane irrespective of ϕ. [c] The first and second values are the electron populations in S_0 and S_1, respectively. Because of the C_2 symmetry, the values on the N^α and N^β atoms are same. [d] The first and second values are the net charges on the N atom in S_0 and S_1, respectively.

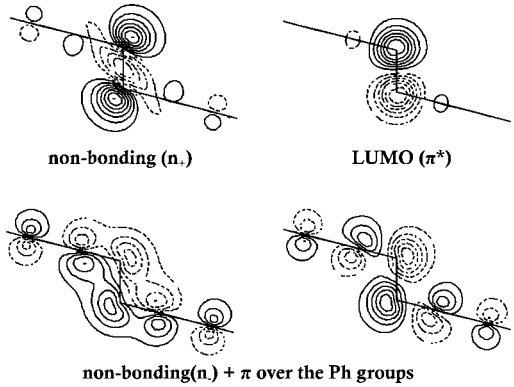

Figure 6. Molecular orbitals relevant to the S_1 state at perpendicularly phenyl twisted conformation. As mentioned in the text, the n_+ and π^* orbitals (in the upper panel) are the main ones used to describe the S_1 state but the other MOs (in the lower panel), where antisymmetric nonbonding orbitals on the P atoms (n_-) highly mix up with the π orbitals over the phenyl groups, are also relatively important.

come to the same conclusion that the geometry of the P═P compound changes little through $n_+-\pi^*$ excitation.

4. Concluding Remarks

In the present paper we compared the P═P double bond character with the N═N one, where we took *t*-DPP and *t*-AZB as model compounds. The electronic structures of *t*-DPP are similar to those of *t*-AZB. However, the phenyl torsional potentials are different from each other, which serves to distinguish the P═P double bond character from the N═N one. In the S_0 state, the torsional potential of *t*-DPP has double wells which lead to nonplanar stable geometries, while that of *t*-AZB has only a single minimum at a planar geometry. This difference is ascribed to the characters of the linkage bonds. The PC linkage bonds have a single bond character, while the NC linkage bonds have somewhat π bond character due to the resonance between the N═N part and the phenyl groups. In the S_1 state, the difference of the phenyl torsional potentials is more drastic. The *t*-AZB potential in S_1 becomes more stiff around a planar conformation. This is ascribed to increase of the double bond character in the NC linkage bond upon $n_+-\pi^*$ excitation. On the other hand, the *t*-DPP potential promotes the phenyl torsion so that the phenyl groups are perpendicularly twisted against the P═P part. The stability of the perpendicularly phenyl twisted conformation can be interpreted by two factors. One is that *t*-DPP has a single bond character even in S_1 ($n_+-\pi^*$) so that the phenyl torsion takes place easily for escape from electronic repulsion between the P═P part and the phenyl groups. The other is that the P═P part is positively charged. Especially in S_1, the in-plane orbitals which contribute to the lone pair orbitals around the P═P part are electron-deficient due to $n_+-\pi^*$ excitation. To compensate for the electron deficiency, the negatively charged phenyl groups are perpendicularly twisted and in consequence the π electron over the phenyl groups effectively transfers into the in-plane orbitals of the P═P part.

Finally we point out that the photochemical behavior of *t*-DPP can possibly be different from that of *t*-AZB. In case of *t*-AZB, for instance, the radiationless relaxation into S_0 takes place even in a confined space where the N═N torsion (not the phenyl torsion in the present study) is prevented. So far several relaxation pathways of *t*-AZB in a confined space have been proposed, though there is still controversy among them.[20] Considering the shape of the phenyl potential surface of *t*-DPP in S_1, the relaxation pathway can possibly be quite different from that of *t*-AZB. Such a theoretical work is in progress.

Acknowledgment. The numerical calculations were partly performed in the Computer Center of Institute for Molecular Science. This work is financially supported by Grant-in-Aid for Priority Area (Molecular Theory for Real Systems; Nos.19029004 and 20038004) from the Ministry of Education, Culture, Sports, Science and Technology.

References and Notes

(1) Yoshifuji, M.; Shima, I.; Inamoto, N.; Hirotsu, K.; Higuchi, T. *J. Am. Chem. Soc.* **1981**, *103*, 4587–4589.
(2) Yoshifuji, M. *J. Chem. Soc., Dalton Trans.* **1998**, 3343–3349.
(3) Twamley, B.; Power, P. P. *Chem.Commun. (Cambridge)* **1998**, 1979–1980.
(4) Twamley, B.; Sofield, C. D.; Olmstead, M. M.; Power, P. P. *J. Am. Chem. Soc.* **1999**, *121*, 3357–3367.
(5) Sasamori, T.; Takeda, N.; Tokitoh, N. *J. Phys. Org. Chem.* **2003**, *16*, 450–462.
(6) Cowley, A. H.; Decken, A.; Norman, N. C.; Krüger, C.; Lutz, F.; Jacobsen, H.; Ziegler, T. *J. Am. Chem. Soc.* **1997**, *119*, 3389–3390.
(7) Weber, L. *Chem. Rev.* **1992**, *92*, 1839–1906.
(8) Power, P. P. *Chem. Rev.* **1999**, *99*, 3463–3503.
(9) Mathey, F. *Angew. Chem., Intl. Ed.* **2003**, *42*, 1578–1603.
(10) Trinquier, G. *J. Am. Chem. Soc.* **1982**, *104*, 6969–6977.
(11) Allan, T. L.; Scheiner, A. C.; Yamaguchi, Y.; Schaefer, H. F., III. *J. Am. Chem. Soc.* **1986**, *108*, 7579–7588.
(12) Nagase, S.; Suzuki, S.; Kurakake, T. *J. Chem. Soc., Chem. Commun* **1990**, 1724–1726.
(13) Mahé, L.; Barthelat, J.-C. *J. Phys. Chem.* **1995**, *99*, 6819–6827.
(14) Cheng, H.; Lin, C.; Chu, S. *J. Phys. Chem. A* **2007**, *111*, 6890–6893.
(15) Kawasaki, S.; Nakamura, A.; Toyota, K.; Yoshifuji, M. *Bull. Chem. Soc. Jpn.* **2005**, *78*, 1110–1120.
(16) Smith, R. C.; Protasiewicz, J. D. *J. Am. Chem. Soc.* **2004**, *126*, 2268–2269.
(17) Hamaguchi, H.; Tasumi, M.; Yoshifuji, M.; Inamoto, N. *J. Am. Chem. Soc.* **1984**, *106*, 508–509.
(18) Copeland, T.; Shea, M. P.; Milliken, M. C.; Smith, R. C.; Protasiewicz, J. D.; Simpson, M. C. *Anal. Chim. Acta* **2003**, *496*, 155–163.
(19) Schmidt, M. W.; Baldridge, K. K.; Boatz, J. A.; Elbert, S. T.; Gordon, M. S.; Jensen, J. H.; Koseki, S.; Matsunaga, N.; Nguyen, K. A.; Su, S. J.; Windus, T. L.; Dupuis, M.; Montgomery, J. A., Jr *J. Comput. Chem.* **1993**, *14*, 1347–1363.
(20) Diau, E. W.-G. *J. Phys. Chem. A* **2004**, *108*, 950–956.

JP8043972